Synthesis, Structure, and Magnetism of $BaVO_{2.8}$: A New Perovskite-Related Vanadate with V^{III}/V^{IV} Ordering

B.-H. Chen,[1a] B. W. Eichhorn,*[1a] H. L. Ju,[1b] and R. L. Greene*[1b]

Center for Superconductivity Research, Departments of Chemistry and Physics, University of Maryland, College Park, Maryland 20742

Received July 21, 1993®

A new barium vanadium oxide, $BaVO_{2.8}$, was prepared from BaO and VO_2 in an evacuated silica ampule at 1100 °C for 10 h with excess Zr getter. The compound consists of interleaving perovskite layers (two corner-sharing VO_6 octahedra) and $BaNiO_3$ type layers (three face-sharing VO_6 octahedra) along the *c*-axis. Curie–Weiss magnetic behavior was observed with $\mu_{eff} = 1.96\ \mu_B$. The structural and magnetic data reveal ordering of V^{III} and V^{IV} cations at the corner-sharing and face-sharing octahedral holes, respectively. Qualitative molecular orbital analysis indicates M–M bonding in the face sharing $[V_3O_{12}]^{12-}$ fragments with net 1/2 bond orders per V–V interaction ($d_{V\text{-}V} = 2.62$ Å). Crystallographic data: hexagonal space group $P\bar{3}m1$; $a = 5.7685(2)$ Å, $c = 11.876(1)$ Å, $V = 342.22(4)$ Å^3, $Z = 5$, and $d_{calc} = 5.65$ g/cm^3. The final *R* factors (Rietveld profile analysis) are $R = 9.37\%$ and $R_{wp} = 10.34\%$.

Introduction

There is current interest in the preparation, structure and properties of the perovskite-related $Sr_{n+1}V_nO_{3n+1}$ Ruddlesden–Popper phases due to their structural similarities to the high T_c copper oxides.[2-5] The strontium vanadates display many of the magnetic and transport properties observed in the high T_c materials (i.e. antiferromagnetic $S = {}^1/_2$ metal ions, metal insulator–transitions, etc.) but possess inverse electronic configurations (d^1 versus d^9). The $n = \infty$ perovskite end member in this family, cubic $SrVO_3$ and its Ca analog $CaVO_3$, are stoichiometric metallic phases that display Pauli paramagnetic behavior.[6-15] The barium vanadate system has been less studied in that the structure of Ba_2VO_4 was only recently described[16] and single phase samples of $BaVO_3$ have not been reported. Many attempted preparations of $BaVO_3$ by different low pressure methods[6,15,17,18] all yielded the highly stable $Ba_3V_2O_8$-type compounds with other unidentified phases. The first $BaVO_3$ phase was prepared by Chamberland and Danielson[6] from BaO and VO_2 at 1200 °C and 60–65 kbar pressure. However, the yield of this compound was approximately 25%, and the exact stoichiometry was unknown. The powder X-ray data indicated the predominant phase possessed a 14-layer hexagonal structure (14H polytype in Ramsdell notation)[19] with $a = 5.6960(7)$ Å and $c = 32.122(9)$ Å. The extra diffraction lines were indexed as a 12-layer rhombohedral structure (a 12R polytype)[19] with $a = 5.726(1)$ Å and $c = 27.821(6)$ Å. Susceptibility measurements on the heterogeneous samples suggested Curie–Weiss paramagnetic behavior with $\mu_{eff} = 1.93$ BM which contrasts with the Pauli paramagnetic behavior of the $CaVO_3$ and $SrVO_3$ phases.

Because of the inconsistency of previous reports concerning the structure and the stoichiometry of $BaVO_3$, a reinvestigation of this system was undertaken. In this paper, we report the synthesis, structure and magnetic properties of single phase oxide $BaVO_{2.8}$. The compound has a $Ba_5Ta_4O_{15}$ related structure with ordered V^{III}/V^{IV} centers and a $[V_3O_{12}]^{12-}$ face sharing trioctahedral fragment.

Experimental Section

The $BaVO_{2.8}$ phase was prepared from a mixture of BaO (460 mg) and VO_2 (249 mg) powders (CERAC Inorganics) in a 1:1 molar ratio. The starting materials were ground and loaded into a 9-mm silica ampule in a N_2 drybox. The 9-mm ampule was placed inside a 12-mm silica ampule containing excess Zr metal (~1 g). The larger ampule was sealed under vacuum and the reaction mixture fired at 1100 °C for 10 h. The sample was cooled to room temperature over a 4-h period, yielding a black polycrystalline powder.

The oxygen content was determined by TGA. The sample was fired in air at 950 °C for 12 h and the white oxidized product analyzed by powder X-ray diffraction.

X-ray powder data for $BaVO_{2.8}$ were obtained by using a modified Phillips XRG2000 diffractometer with Cu Kα radiation interfaced with a RADIX databox and a MDI software system. Data were collected in the range $20° \le 2\theta \le 80°$ with the step width of 0.02° and a count rate of 20 seconds. The $BaVO_{2.8}$ phase was successfully refined by Rietveld analysis under hexagonal symmetry $P\bar{3}m1$ with Pearson VII profile shape functions. The coordinates of $BaCrO_{2.9}$ were used as the starting model.[20]

The dc magnetic susceptibility of $BaVO_{2.8}$ was measured between 4 and 300 K and an applied field of 300 G by using a Quantum Design SQUID magnetometer. The 43 mg pelletized sample was suspended in the cavity of the magnetometer by dental floss. The sample was cooled to 4 K, the magnetic field applied, and the magnetization measured as the temperature was raised to 300 K (i.e. zero-field cooled). In a separate experiment, the magnetization of the sample was measured from 300 down to 4 K (i.e. field cooled).

Qualitative extended Hückel molecular orbital calculations[21] were performed on a $V_3(OH)_{12}$ model employing standard ionization potentials

• Abstract published in *Advance ACS Abstracts*, October 15, 1993.

(1) (a) Department of Chemistry. (b) Department of Physics.
(2) Rey, M. G.; Dehaudt, Ph.; Joubert, J. C.; Lambert-Andron, B.; Croyt, M.; Croyt-Lackmann, F. *J. Solid State Chem.* **1990**, *86*, 101.
(3) Itoh, M.; Shikano, M.; Liang, R.; Kawaji, H.; Nakamura, T. *J. Solid State Chem.* **1990**, *88*, 597.
(4) Gong, W., Xue, J. S., Greedan, J. E. *J. Solid State Chem.* **1991**, *91*, 180.
(5) Nozaki, A.; Yoshikawa, H; Wada, T.; Tamauchi, H.; Tanaka, S. *Phys. Rev. B* **1991**, *43*, 181.
(6) Chamberland, L.; Danielson, P. S. *J. Solid State Chem.* **1971**, *3*, 243.
(7) Deduit, J. *Ann. Chim Paris* **1961**, *6*, 163.
(8) (a) Reuter, B.; Wallnik, M. *Naturwissenschaften* **1963**, *50*, 569. (b) Reuter, B. *Bull Soc. Chim. Fr.* **1965**, 1053.
(9) Wollnik, M. Ph.D. Thesis, Technical University of Berlin, 1965.
(10) Roth, R. S. *J. Res. Natl. Bur. Stand.* **1957**, *58*, 75.
(11) Rudorff, W.; Walter, G.; and Becker, H. *Z. Anorg. Allg. Chem.* **1956**, *285*, 287.
(12) Klarding, J. *Z. Anorg. Allg. Chem.* **1944**, *252*, 190.
(13) Kestigian, M. J.; Dickinson, J. G.; Ward, R. *J. Am. Chem. Soc.* **1957**, *79*, 5598.
(14) Rudorff, W.; Reuter, B. *Z. Anorg. Allg. Chem.* **1947**, *253*, 177.
(15) Palanisamy, T.; Gopalakrishnan, J.; Sastri, M. V. C. *Z. Anorg. Allg. Chem.* **1975**, *415*, 275.
(16) Liu, G.; Greedan, J. E. *J. Solid State Chem.* **1993**, *103*, 228.
(17) Gushee, B. E.; Katz, L.; Ward,R. *J. Am. Chem. Soc.* **1957**, *79*, 5601.
(18) (a) Spitsbergen, U. Ph.D. Thesis, University of Leiden, 1962. (b) Feltz, A.; Schmalfuss, S. *Krist. Tech.* **1971**, *6*, 367.
(19) (a) Ramsdell, L. S. *Am. Mineral.* **1947**, *32*, 64. (b) Ramsdell, L. S.; Kohn, J. A. *Acta Cryst.* **1951**, *4*, 111.
(20) Torii, Y. *Chem. Lett.* **1975**, 557.
(21) Hoffmann, R. *J. Chem. Phys.* **1963**, *39*, 1397.

0020-1669/93/1332-5715$04.00/0

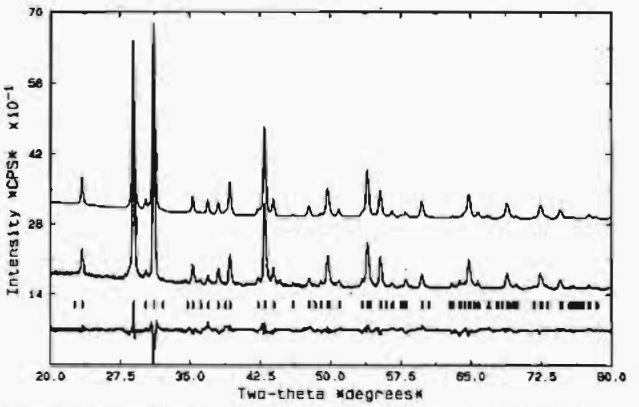

Figure 1. Reitveld profile refinement of powder X-ray data for $BaVO_{2.8}$. The calculated and experimental profiles are shown at the top and middle, respectively, with the difference profile shown at the bottom (same scale).

Table I. Summary of Crystallographic Data for $BaVO_{2.8}$

space group	$P\bar{3}m1$ (No. 164)	Z	5
a (Å)	5.7685(2)	ρ (g/cm^3)	5.65
c (Å)	11.876(1)	R (%)[a]	9.37
V (Å^3)	342.22(4)	R_{wp} (%)[b]	10.34

[a] $R = 100\{[\sum(I_{obs} - I_{cal})^2]/[\sum(I_{obs})^2]\}^{1/2}$. [b] $R_{wp} = 100\{[\sum w(I_{obs} - I_{cal})^2]/[\sum w(I_{obs})^2]\}^{1/2}$.

Table II. Fractional Coordinates for $BaVO_{2.8}$

atom	site	x	y	z
Ba(1)	1a	0	0	0
Ba(2)	2d	$^1/_3$	$^2/_3$	0.7821(4)
Ba(3)	2d	$^1/_3$	$^2/_3$	0.4287(4)
V(1)	2d	$^1/_3$	$^2/_3$	0.1095(9)
V(2)	2c	0	0	0.2797(9)
V(3)	1b	0	0	$^1/_2$
O(1)	3e	$^1/_2$	0	0
O(2)	6i	0.169(5)	$-x$	0.204(3)
O(3)	6i	0.183(3)	$-x$	0.611(3)

and exponents as basis functions.[22] Crystallographically determined V–V and V–O distances and angles of the $[V_3O_{12}]^{12-}$ subunit in $BaVO_{2.8}$ were used to construct the $V_3(OH)_{12}$ model. Hydrogen atoms were added to all oxygen atoms and were placed at idealized positions (d_{O-H} = 0.96 Å). All calculations were conducted on a CAChe computational system. Under D_{3d} symmetry, the 15 vanadium 3d orbitals transform as $2a_{1g} + 4e_g + 1a_{2u} + 2e_u$. Six orbitals were V–O σ^* in nature ($2e_g + e_u$) whereas the remainder constituted the V–V σ, nonbonding, and σ^* interactions.

Results and Discussion

The new barium vanadium oxide phase $BaVO_{2.8}$ was prepared from BaO and VO_2 at 1100 °C in the presence of excess Zr getter. The indexed powder X-ray diffraction data yield cell parameters indicative of a $Ba_5Ta_4O_{15}$ type structure[23] (see below) although the stoichiometry revealed a 1:1 ratio of Ba to V. Attempted preparations of $Ba_5V_4O_{15-\delta}$ from 5:4 ratios of BaO to VO_2 produced $BaVO_{3-\delta}$ and large quantities of unidentified phases whereas stoichiometric 1:1 ratios of BaO to VO_2 yielded single phase $BaVO_{3-\delta}$. In addition, structural refinements of the single phase product were attempted by using both $Ba_5V_4O_{15-\delta}$ and $BaVO_{3-\delta}$ models (see below) with the latter giving the lowest final residuals. The oxygen content was determined to be $BaVO_{2.80(6)}$ by TGA studies. The oxidized product from the TGA analysis was identified as single phase $Ba_2V_2O_7$. Under our preparatory conditions, the oxygen content of the phase is invariant in that the compound cannot be prepared in the absence of a Zr getter and excess Zr does not reduce the compound beyond $BaVO_{2.8}$. The composition of $BaVO_{2.8}$ requires an average vanadium oxidation state of +3.6 with a formal V^{III}/V^{IV} mixed valency.

(22) (a) Carlson, T. A. *Photoelectron and Auger Spectroscopy*; Plenum Press: New York, 1975. (b) Ballhausen, C. J.; Gray, H. B. *Molecular Orbital Theory*; W. A. Benjamin, Inc. 1965.
(23) Galasso, F.; Katz, L. *Acta Crystallogr.* **1961**, *14*, 647.

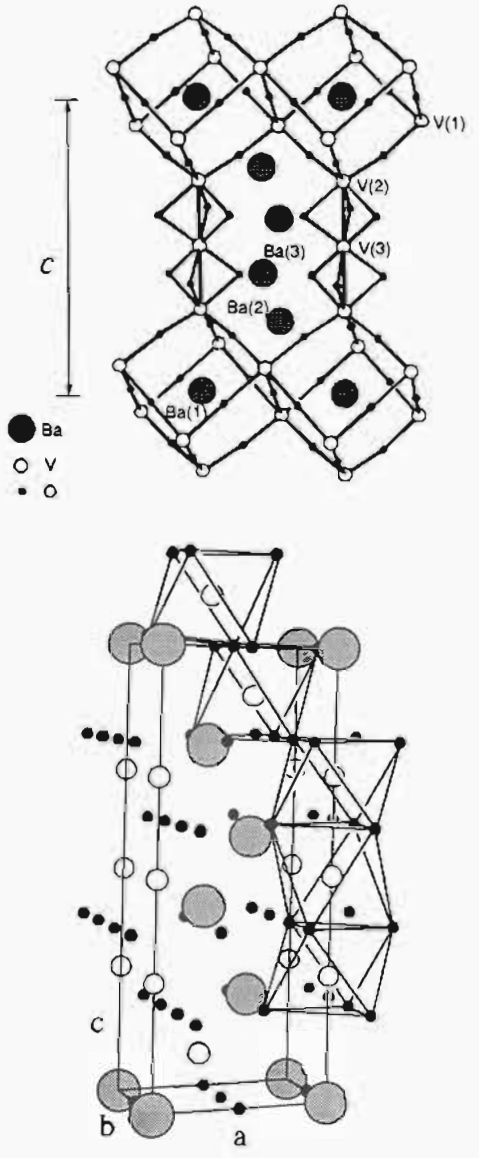

Figure 2. Schematic ball-and-stick drawings of the $BaVO_{2.8}$ structure showing (a, top) face-sharing and corner-sharing portions of the structure and (b, bottom) the orientation of the VO_6 octahedra in the unit cell.

Table III. Selected Interatomic Distances (Å) for $BaVO_{2.8}$

V(2)–V(3)	2.62(1)	Ba(3)–O(3)	2.64(8)
Ba(1)–O(1)	2.8842(2)	Ba(3)–O(3)	2.93(4)
Ba(1)–O(2)	2.96(7)	V(1)–O(1)	2.11(1)
Ba(2)–O(1)	3.078(8)	V(1)–O(2)	1.99(7)
Ba(2)–O(2)	2.89(6)	V(2)–O(2)	1.91(7)
Ba(2)–O(3)	2.53(6)	V(2)–O(3)	2.24(6)
Ba(3)–O(2)	3.13(7)	V(3)–O(3)	2.25(6)

The structure of $BaVO_{2.8}$ is a modified $Ba_5Ta_4O_{15}$-type[23] comprising a 1:1 ratio of Ba to V and ordered V^{III} and V^{IV} ions. The structure was determined by Rietveld profile refinement from X-ray powder data by using a modified $Ba_5Ta_4O_{15}$ model (see Figure 1). The occupancy factors of oxygen were arbitrarily fixed at 0.933 (corresponding to $BaVO_{2.8}$) due to the difficulty of refining oxygen parameters from powder X-ray data. Two polyhedral representations of the structure are given in Figure 2. A summary of the crystallographic parameters and atomic coordinates is given in Tables I and II. The selected interatomic distances for $BaVO_{2.8}$ are listed in Table III and a comparison of the structures of $BaVO_{2.8}$ and the parent $Ba_5Ta_4O_{15}$ is given in Figure 3.

The parent compound $Ba_5Ta_4O_{15}$ has hexagonal symmetry $P\bar{3}m1$ with a = 5.79 Å, c = 11.75 Å, and V = 341.1 Å^3 and is designated a 5H polytype.[19] Four other closely related ternary

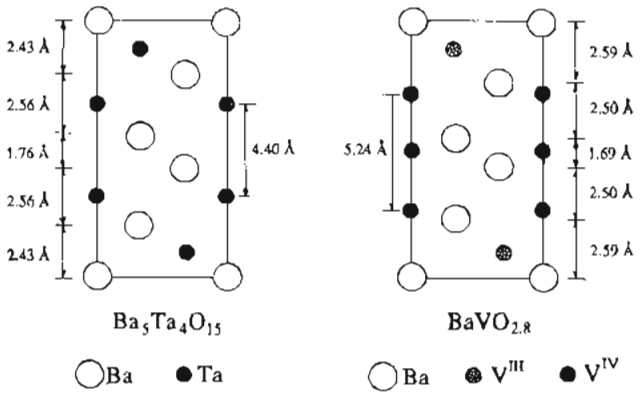

Figure 3. Comparative [110] projections of the $Ba_5Ta_4O_{15}$ and $BaVO_{2.8}$ structures. The separations between BaO_3 layers are shown on the outside of the drawings with the M–M separations shown on the inside (M = Ta, V).

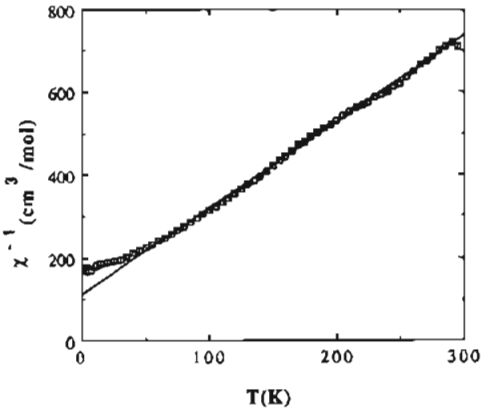

Figure 4. Plot of reciprocal molar magnetic susceptibility versus temperature from 300 to 4 K. The squares show the experimental data and the line represents the best least squares fit.

phases $Ba_5Nb_4O_{15}$, $Sr_5Ta_4O_{15}$, and $Eu_5M_4O_{15}$ (M = Ta, Nb) also adopt this structure.[23,24] These compounds comprise five closest packed AO_3 layers stacked perpendicular to the *c*-axis with a *ccchh* stacking sequence. The B-site ions occupy octahedral voids between these layers but are systematically absent between the two hexagonal closest packed layers, i.e. the 1b Wykoff site at (0, 0, $^1/_2$). To our knowledge, $BaCrO_{2.9}$ is the only other phase that adopts this 5H polytype[20] but has full occupation of the 1b sites in contrast to the other $A_5B_4O_{15}$ compounds. $BaVO_{2.8}$ was refined using both $Ba_5Ta_4O_{15}$ (with 20% random BaO vacancies) and $BaCrO_{2.9}$ models which yielded R (R_w) values of 0.1023 (0.1089) and 0.976 (0.1034), respectively. The refined V(2)–V(2) distances of 5.24 Å for the latter model and 5.60 Å for the former model are both substantially longer than the Ta(2)–Ta(2) separation[23] of 4.40 Å found for $Ba_5Ta_4O_{15}$ (see Figure 3). These data, together with the stoichiometry studies described previously, clearly indicate that $BaVO_{2.8}$ possesses a $BaCrO_{2.9}$ structure type with a fully occupied 1b site.

The *ccchh* packing in $BaVO_{2.8}$ results in the formation of isolated $[V_3O_{12}]^{12-}$ subunits comprising three face-sharing VO_6 octahedra with V–V contacts of 2.62(1) Å. The V_3O_{12} subunits are oriented parallel to the *c* axis and are separated by two layers of corner-sharing octahedra (Figure 2a). The structure can be viewed as a $BaNiO_3$ block[25] (three face-sharing octahedra) separated by a perovskite block (two corner-sharing octahedra). The perovskite layer is tipped such that the 111 direction of the idealized cubic perovskite cell (*Pm3m*) is parallel to the *c* axis in $BaVO_{2.8}$. The Ba–O and V–O contacts (Table III) are similar to those of related compounds[2-5,16] but are not reliable due to the inaccuracy of refining oxygen positions in a Rietveld X-ray analysis.

The structural and magnetic data for $BaVO_{2.8}$ are consistent with the ordering of V^{III} and V^{IV} ions in the corner-sharing and face-sharing sites, respectively. The distances between the BaO_3 layers hosting the face-sharing octahedra are 1.69 (2) Å (*hh* separation) and 2.50 (2) Å (*ch* separation) which are similar to the 1.76- and 2.56-Å separations observed[23] in $Ba_5Ta_4O_{15}$ as shown in Figure 3. The separation between BaO_3 layers hosting the corner-sharing octahedra (*cc* separation) is 2.59 (1) Å which is greater than the 2.43 Å separation found for $Ba_5Ta_4O_{15}$. The increased *cc* layer separation in $BaVO_{2.8}$ may be due to the lower charge of V^{III} (versus Ta^V) which would increase the coulombic repulsions between the negatively charged BaO_3 layers. The ionic radii of V^{III} and Ta^V are both 0.78 Å.[26] The V^{IV} ions occupy face-sharing octahedral sites which, at a V–V separation of 2.62 (1) Å, results in localized M–M bonding (see below). The formation of V–V bonds between *hh* and *ch* layers is consistent with the slight decrease in the BaO_3 interlayer separation relative to $Ba_5Ta_4O_{15}$ (see Figure 3). This ordered structural model requires a stoichiometry of $BaVO_{2.8}$ with three V^{IV} and two V^{III} ions per unit cell which is in excellent agreement with the TGA data and the observed magnetic susceptibility studies.

The plot of reciprocal magnetic susceptibility versus temperature (zero field cooled) for $BaVO_{2.8}$ is presented in Figure 4. The compound exhibits Curie–Weiss paramagnetic behavior[27] over a large temperature range. A least squares fitting of the data between 50 and 300 K gave C = 0.48 cm^3 K/mol, Θ = –53 K and a negligible temperature independent component. Below 50 K there appears to be antiferromagnetic ordering as evidenced by the positive deviation from Curie–Weiss behavior in the plot of reciprocal susceptibility versus temperature (Figure 4). The onset of antiferromagnetism below 50 K is consistent with the Weiss temperature (Θ = –53 K). To confirm the antiferromagnetism and to understand the antiferromagnetic transition in more detail, a neutron scattering experiment is required. The field cooled susceptibility shows a *negative* departure from Curie–Weiss behavior due to low level ferromagnetic impurities; however, both field-cooled and zero-field-cooled susceptibilities are identical in the Curie–Weiss region.

The effective magnetic moment can be extracted from the Curie constant according to

$$C = \frac{N\mu_{eff}^2}{3k_B}$$

where N is Avogadro's number, k_B is Boltzman's constant, and μ_{eff} is the effective magnetic moment in Bohr magnetons (μ_B). From the Curie constant, one calculates an effective magnetic moment of 1.96 μ_B per vanadium for $BaVO_{2.8}$. This value is similar to that reported for the high pressure "$BaVO_3$" phase (1.93 μ_B)[6] but higher than the theoretical spin-only value of 1.73 μ_B for V^{IV} as expected. However, this value is substantially lower than the expected moment based on noninteracting mixed valent V^{III}/V^{IV} model. By using spin-only moments, μ_s, for V^{III} (2.83 μ_B) and V^{IV} (1.73 μ_B) to construct a magnetic model, the observed μ_{eff} can be estimated from the weighted average of the three V^{IV} and two V^{III} ions in the lattice. From the equation

$$\mu_{eff} = \sqrt{^2/_5\mu_s^2(V^{III}) + ^3/_5\mu_s^2(V^{IV})}$$

one calculates a moment of 2.24 μ_B for the noninteracting model.

(24) Fayolle, J.-P.; Raveau, B. *C. R. Seances Acad. Sci. Ser. C* **1974**, *279*, 521.
(25) For general description of structure types, see: Rao, C. N. R.; Gopalakrishnan, J. *New Directions in Solid State Chemistry*; Cambridge University Press: Cambridge, England, 1986.
(26) Shannon, R. D. *Acta Crystallogr.* **1976**, *A32*, 751.
(27) Kittel, C. *Introduction to Solid State Physics* 6th ed., Wiley and Sons: New York, 1986; p 424.

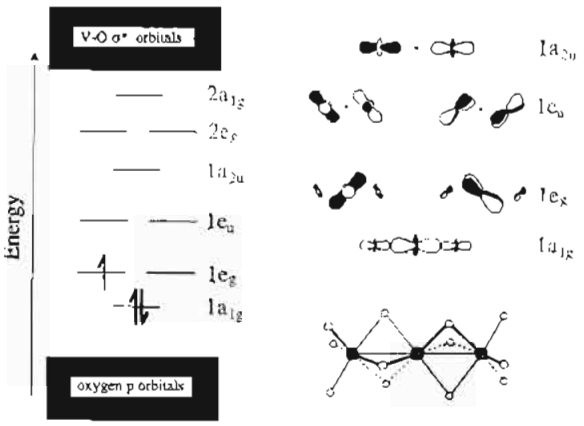

Figure 5. Qualitative molecular orbital diagram and canonical representations of selected orbitals for $V_3(OH)_{12}$. The V–V and V–O distances and angles were taken from the $[V_3O_{12}]^{12-}$ fragment in $BaVO_{2.8}$.

If one considers the localized M–M bonding between the three face-sharing vanadium atoms, a pairing of electrons in a covalent three-center/three-electron interaction is observed. Results of a qualitative molecular orbital calculation on a $V_3(OH)_{12}$ model representing the $[V_3O_{12}]^{12-}$ subunit in $BaVO_{2.8}$ are shown in Figure 5. The V_3O_{12} core (I) possesses D_{3d} point symmetry and

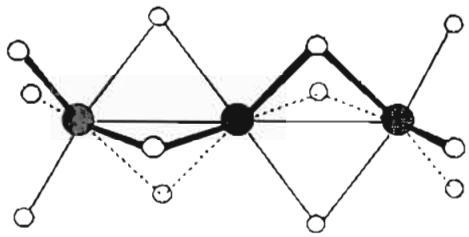

I

contains three metal based electrons from the three V^{IV} centers. One finds a V–V σ-bonding orbital ($1a_{1g}$) derived from the in-phase combination of the three d_{z^2} atomic orbitals as the lowest energy metal based molecular orbital. The next highest MO's are a degenerate e_g set of hybridized d_{xz} and d_{yz} type orbitals that are primarily localized on the central vanadium and possess minimal M–M σ- and π-like character (Figure 5). Five essentially nonbonding orbitals ($1e_u$, $2e_g$, and $1a_{2u}$) and one M–M antibonding orbital ($2a_{1g}$) lie at higher energy and are unoccupied. The orbital picture is analogous to that described for $[Ru_3Cl_{12}]^{4-}$ and related compounds[28,29] with the exception of the ordering of some of the nonbonding orbitals. The three d electrons from the three V^{IV} ions fill the $1a_{1g}$ orbital and leave one unpaired electron in the $1e_g$ orbital pair (Figure 5). The vanadium–vanadium bonding results in the formation of a net half-bond per V–V interaction (assuming the e_g orbital is nonbonding) and one unpaired electron per $[V_3O_{12}]^{12-}$ subunit. The V–V separation of 2.62(1) Å is less than the sum of two covalent single-bond radii for vanadium (1.346 Å), which is indicative of a direct metal–metal interaction.[30] A comparison with other related complexes is given below.

If the lone $1e_g$ electron is approximated as a single d^1 ion with $\mu_s = 1.73\ \mu_B$, the expected magnetic moment can be described by the following equation:

$$\mu_{eff} = \sqrt{{}^2/_5\mu_s^2(V^{III}) + {}^1/_5\mu_s^2([V_3O_{12}])}$$

The assumption that the electron in the V_3O_{12} subunit contributes a spin-only moment is based on comparisons with molecular divanadium and trivanadium compounds where orbital contributions to the effective moments are negligible[31] and the $S = {}^1/_2$ $[W_2X_9]^{2-}$ ions (X = Cl, Br)[32] with $\mu_{eff} = 1.72$–$1.87\ \mu_B$. On the basis of the M–M bonded model, one calculates a moment of 1.95 BM for $BaVO_{2.8}$, which is in excellent agreement with the experimental data. Interchanging the positions of the V^{III} and V^{IV} ions in the structure would result in an expected μ_{eff} of much less than 1.73 μ_B per vanadium.

It is informative to examine M–M bond distances in related compounds in order to assess the degree of V–V bonding in the V_3O_{12} fragment. The series of $Cs_3M_2Cl_9$ compounds (M = Ti, V, Cr, Mo, Ru)[33-35] containing face-sharing bioctahedral $[M_2Cl_9]^{3-}$ units provides a useful comparison. Structural and magnetic studies on $Cs_3Ru_2Cl_9$ (Ru^{III}) reveal a strong direct Ru–Ru bond[33] ($d_{Ru-Ru} = 2.725$ Å) which is consistent with subsequent theoretical studies.[29] The linear face sharing trioctahedral complexes[28] $[Ru_3Cl_{12}]^{4-}$ (2 Ru^{III}, Ru^{II}) and $[Ru_3Cl_8(PEt_3)_4]^+$ (Ru^{III}) also contain direct Ru–Ru bonds ($d_{Ru-Ru} = 2.805(1)$ and 2.906(3) Å, respectively) but with formal bond orders of ${}^1/_2$. In contrast, the $[M_2Cl_9]^{3-}$ions where M = Ti, V, and Cr[34] display long metal–metal separations ranging between 3.191 Å (Ti) and 3.317 Å (Cr) with no direct M–M bonding. Although $Cs_3V_2Cl_9$ has not been structurally characterized, it is known to be isomorphic to the Cr and Ti analogs and has virtually identical lattice parameters.[34,36] Therefore, one can assume that the V–V separation will be approximately 3.2 Å in $Cs_3V_2Cl_9$. The V–V contacts in the V_3O_{12} subunits of $BaVO_{2.8}$ are over 0.5 Å shorter and are similar to Mo^V–Mo^V single bond distances[37] and the Mo–Mo separation in $Cs_3Mo_2Cl_9$ ($d_{Mo-Mo} = 2.65$ Å).[34] Vanadium-to-vanadium separations where direct M–M bonding has been implicated range from 1.978 (2) (V≡V)[38] to 2.73 Å (V=V).[39] Thus, despite the high oxidation state of vanadium in the V_3O_{12} subunits which leads to contracted V 3d orbitals, structural and magnetic studies indicate direct M–M bonding.

The three-dimensional perovskite d^1 vanadium oxides $CaVO_3$ and $SrVO_3$ are metallic[7-16] as are the one-dimensional d^1 compounds $BaVS_3$ and $BaVSe_3$ with $BaNiO_3$ structure types.[40,41] The $BaNiO_3$/perovskite composite $BaVO_{2.8}$, however, is semiconducting which is presumably due to a combination of structural and electronic effects. The V_3O_{12} subunit displays highly localized metal–metal bonding and would not be expected to possess itinerant electrons. Likewise, the d^2 V^{III} ions in the two dimensional perovskite blocks are analogous to the d^2 RVO_3 perovskite materials (R = rare earth) which are magnetic insulators.[42] Thus, the isolation of the V_3O_{12} subunits in the hexagonal region and the electronic localization in the V^{III} ions

(28) (a) Bino, A.; Cotton, F. A. *J. Am. Chem. Soc.* **1980**, *102*, 608. (b) Cotton, F.A.; Matusz, M.; Torralba, R. C. *Inorg. Chem.* **1989**, *28*, 1516. (c) Cotton, F.A.; Torralba, R. C. *Inorg. Chem.* **1991**, *30*, 3293.
(29) Bursten, B. E.; Cotton, F. A.; Fang, A. *Inorg. Chem.* **1983**, *22*, 2127.
(30) Pearson, W. B. *The Crystal Chemistry and Physics of Metals and Alloys*; Wiley-Interscience, New York, 1972, pp 146–152.
(31) (a) Edema, J. J. H.; Gambarotta, S.; Hao, S.; Bensimon, C. *Inorg. Chem.* **1991**, *30*, 2586. (b) Gelmini, L; Armstrong, W. H. *J. Chem. Soc., Chem. Commun.* **1989**, 1904.
(32) Saillant, R.; Wentworth, R. A. D. *J. Am. Chem. Soc.* **1969**, *91*, 2174.
(33) Darriet, J. *Rev. Chim. Miner.* **1981**, *18*, 27.
(34) (a) Saillant, R.; Hayden, J. L.; Wentworth, R. A. D. *Inorg. Chem.* **1967**, *6*, 1497. (b) Saillant, R.; Wentworth, R. A. D. *Inorg. Chem.* **1969**, *8*, 1226. (c) Saillant, R.; Jackson, R. B.; Streib, W. E.; Folting, K; Wentworth, R. A. D. *Inorg. Chem.* **1971**, *10*, 1453.
(35) Brait, B.; Kahn, O.; Morgenstein-Badarau, I; Rivoal, J. C. *Inorg. Chem.* **1981**, *20*, 4193.
(36) Powder X-ray diffraction data reindexed by the Joint Commission on Powder X-ray Diffraction. See JCPDS cards No. 21–230 ($Cs_3Ti_2Cl_9$) hexagonal ($P6_3/mmc$), $a = 7.32$ Å; $c = 17.97$ Å; No. 21–233 ($Cs_3V_2Cl_9$) hexagonal ($P6_3/mmc$), $a = 7.24$ Å; $c = 17.94$ Å; No. 21–205 ($Cs_3Cr_2Cl_9$) hexagonal ($P6_3/mmc$), $a = 7.22$ Å, $c = 17.93$ Å.
(37) (a) Spivack, B.; Ganghan, A. P.; Dori, Z. *J. Am. Chem. Soc.* **1971**, *93*, 5266. (b) Brown, D. H.; Jeffreys, J. A. D. *J. Chem. Soc., Dalton Trans.* **1973**, 732.
(38) (a) Cotton, F. A.; Daniels, L. M.; Murillo, C. A. *Angew. Chem., Int. Ed. Engl.* **1992**, *31*, 737. (b) Cotton, F. A.; Millar, M. *J. Am. Chem. Soc.* **1977**, *99*, 7886.
(39) (a)Vahrenkamp, H. *Chem. Ber.*, **1978**, *111*, 3472. (b) Huffman, J. C.; Lewis, L.N.; Caulton, K. G. *Inorg. Chem.* **1980**, *19*, 1137.
(40) Gardner, R. A.; Vlasse, M.; Wold, A. *Acta Crystallogr.* **1969**, *B25*, 781.
(41) Kelber, J.; Reis Jr., A. H.; Aldred, A. T.; Mueller, M. H.; Massenet, O.; Depasquali, G.; Stucky, G. *J. Solid State Chem.* **1979**, *30*, 357.

of the perovskite region render $BaVO_{2.8}$ semiconducting in contrast to the related AVX_3 members of the series.

In the summary, hexagonal $BaVO_{2.8}$ was prepared for the first time and displays a modified $Ba_5Ta_4O_{15}$ structure type with ordered V^{III} / V^{IV} ions. Structural and magnetic data reveal a V_3O_{12} subunit (V^{IV} ions) with localized V–V bonding and a perovskite block containing V^{III} ions. $BaVO_{2.8}$ appears to be the most accessible phase in the $BaVO_{3-\delta}$ system and is not amenable to changes in oxygen content. In contrast, the perovskite $SrVO_3$ and $CaVO_3$ phases can be prepared as oxygen precise materials.

(42) (a) Shin-Ike, T.; Sakai, T.; Adachi G.; Shiokawa, J. *Mater. Res. Bull.* **1976**, *11*, 801. (b) Mahafan, A. V.; Johnston, D. C.; Torgeson, D. R.; Borsa, F. *Phys. Rev. B* **1992**, *46*, 10966 and references therein.

Acknowledgment. This work was supported by the National Science Foundation (DMR-8913906), the Center for Superconductivity Research and the Department of Chemistry and Biochemistry at the University of Maryland. We are grateful to Dr. J. Peng for helpful discussions concerning the magnetic data and a reviewer for suggesting a Pauling Bond Order analysis.